

A slope-based decoupling algorithm to simultaneously control dual deformable mirrors in a woofer-tweeter adaptive optics system

Tao Cheng(程涛), Wenjin Liu(刘文劲), Boqing Pang(庞博清), Ping Yang(杨平), Bing Xu(许冰)

Citation: Chin. Phys. B . 2018, 27(7): 070704. **doi:** 10.1088/1674-1056/27/7/070704

Journal homepage: http://cpb.iphy.ac.cn; http://iopscience.iop.org/cpb

What follows is a list of articles you may be interested in

Elastic strain response in the modified phase-field-crystal model

Wenquan Zhou(周文权), Jincheng Wang(王锦程), Zhijun Wang(王志军), Yunhao Huang(黄赟浩), Can Guo(郭灿), Junjie Li(李俊杰), Yaolin Guo(郭耀麟)

Chin. Phys. B . 2017, 26(9): 090702. **doi:** 10.1088/1674-1056/26/9/090702

Effective transport of passive particles induced by chiral-active particles in microchannel

Yunfeng Hua(华昀峰), Linli He(何林李), Linxi Zhang(章林溪)

Chin. Phys. B . 2017, 26(8): 080702. **doi:** 10.1088/1674-1056/26/8/080702

Co-focus experiment of segmented mirror

Bin Li(李斌), Wen-Hao Yu(于文豪), Mo Chen(陈莫), Jin-Long Tang(唐金龙), Hao Xian(鲜浩)

Chin. Phys. B . 2017, 26(6): 060706. **doi:** 10.1088/1674-1056/26/6/060706

High signal-to-noise ratio sensing with Shack-Hartmann wavefront sensor based on auto gain control of electron multiplying CCD

Zhao-Yi Zhu(朱召义), Da-Yu Li(李大禹), Li-Fa Hu(胡立发), Quan-Quan Mu(穆全全), Cheng-Liang Yang(杨程亮), Zhao-Liang Cao(曹召良), Li Xuan(宣丽)

Chin. Phys. B . 2016, 25(9): 090702. **doi:** 10.1088/1674-1056/25/9/090702

Molecular modeling of oscillating GHz electric field influence on the kinesin affinity to microtubule

H. R. Saeidi, S. S. Setayandeh, A. Lohrasebi

Chin. Phys. B . 2015, 24(8): 080701. **doi:** 10.1088/1674-1056/24/8/080701

A slope-based decoupling algorithm to simultaneously control dual deformable mirrors in a woofer–tweeter adaptive optics system*

Tao Cheng(程涛)[1,2,3], Wenjin Liu(刘文劲)[1,3], Boqing Pang(庞博清)[1,2,3], Ping Yang(杨平)[1,3,†], and Bing Xu(许冰)[1,3]

[1] *Key Laboratory on Adaptive Optics, Chinese Academy of Sciences, Chengdu* 610209, *China*
[2] *University of Chinese Academy of Sciences, Beijing* 100049, *China*
[3] *Institute of Optics and Electronics, Chinese Academy of Sciences, Chengdu* 610209, *China*

(Received 30 December 2017; revised manuscript received 2 May 2018; published online 25 June 2018)

We propose a slope-based decoupling algorithm to simultaneously control the dual deformable mirrors (DMs) in a woofer–tweeter adaptive optics system. This algorithm can directly use the woofer's response matrix measured from a Shack–Hartmann wave-front sensor to construct a slope-based orthogonal basis, and then selectively distribute the large-amplitude low-order aberration to woofer DM and the remaining aberration to tweeter DM through the slope-based orthogonal basis. At the same moment, in order to avoid the two DMs generating opposite compensation, a constraint matrix used to reset tweeter control vector is convenient to be calculated with the slope-based orthogonal basis. Numeral simulation demonstrates that this algorithm has a good performance to control the adaptive optics system with dual DMs simultaneously. Compared with the typical decoupling algorithm, this algorithm can take full use of the compensation ability of woofer DM and release the stroke of tweeter DM to compensate high-order aberration. More importantly, it does not need to measure the accurate shape of tweeter's influence function and keeps better performance of restraining the coupling error with the continuous-dynamic aberration.

Keywords: dual deformable mirrors, decoupling algorithm, adaptive optics

PACS: 07.05.Tp, 95.75.Qr, 42.68.Wt **DOI:** 10.1088/1674-1056/27/7/070704

1. Introduction

Adaptive optics is a very efficient technology used to correct the wave-front aberration, so it has been successfully used in the laser beam shaping systems, telescopes, and vision instruments.[1–3] However, to achieve better correction performance, adaptive optics system should compensate both low-order and high-order wave-front aberration simultaneously. Though many researchers have done a lot of study about large stroke and high spatial frequency deformable mirror (DM), the application of this DM still need solve many technological problems.[4] So the woofer–tweeter adaptive optics system shown in Fig. 1 is really an efficient solution to simultaneously compensate phase distortion with a large amplitude and high spatial frequency, where the woofer is used to correct the large stroke and low spatial frequency aberration and the tweeter is used to correct low stroke and high spatial frequency aberration.

From Fig. 1, the residual wave-front is measured by a single wave-front sensor (WFS) and distributed to the dual DMs with some specified methods. However, different from a single-DM adaptive optics system, the woofer–tweeter system must face the cross-couple between the dual DMs, which may induce a serious waste of the DMs' correction ability and even destroy the system stability.[5] Several algorithms have been proposed to control the dual DMs, such as two-step control algorithm,[6–8] Zernike mode decomposition algorithm,[9–11] Fourier mode decomposition algorithm,[12] wavelet mode decomposition algorithm,[13] Lagrange-multiplier damped least-squares algorithms,[14–16] and direct slope-based correction algorithm.[17] But the algorithm which can effectually suppress the coupling errors between the two DMs is very few. So far, the two-step algorithm and Zernike mode decomposition algorithm can get better performance to restrain coupling error between the dual DMs. However, the two-step algorithm is unable to correct the dynamic aberration, and the Zernike mode decomposition algorithm must reconstruct the wave-front by the Zernike mode and measure the accurate influence function of tweeter DM to construct a constraint matrix. In the practical process, the accurate shape of tweeter's influence function is often measured by the interferometer or fitted by Zernike mode. This process is complicated, but indispensable.

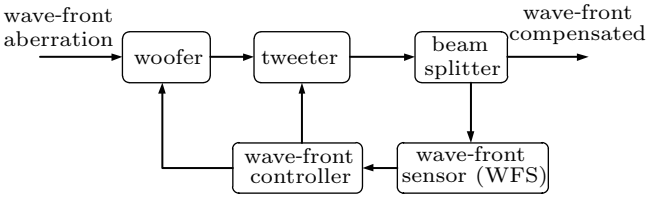


Fig. 1. The woofer–tweeter adaptive optics system.

*Project supported by the Key Scientific Equipment Development Project of China (Grant No. ZDYZ2013-2), the National High-Tech R&D Program of China (Grant Nos. G128201-G158201 and G128603-G158603), the Innovation Fund of Chinese Academy of Science (Grant No. CXJJ-16M208), the Youth Innovation Promotion Association of the Chinese Academy of Sciences, and the Outstanding Young Scientists, Chinese Academy of Sciences.

†Corresponding author. E-mail: pingyang2516@163.com

© 2018 Chinese Physical Society and IOP Publishing Ltd

In this paper, we propose a slope-based decoupling algorithm to simultaneously control dual DMs. Compared with the typical decoupling algorithm, this algorithm can take full use of the compensation ability of woofer DM and release the stroke of tweeter DM to correct the high spatial frequency aberration. In addition, this algorithm can construct the constraint matrix used to reset the command vectors of tweeter DM without measuring the accurate influence function, and can keep better performance of restraining the coupling error with the continuous-dynamic aberration.

2. Principle of slope-based decoupling algorithm

In the woofer–tweeter adaptive optics system, the response matrix of woofer $\boldsymbol{D}_{\mathrm{W}}(2n\times m_1)$ and tweeter $\boldsymbol{D}_{\mathrm{T}}(2n\times m_2)$ can be measured by a Shack–Hartmann wavefront sensor, where n is the number of Hartmann's aperture, and m_1 and m_2 are the numbers of actuator of woofer and tweeter DMs, respectively. The slope of wave-front $\boldsymbol{g}(2n\times 1)$ representing residual errors can be corrected by dual DMs as

$$\boldsymbol{g}=\boldsymbol{D}_{\mathrm{W}}\boldsymbol{V}_{\mathrm{W}}+\boldsymbol{D}_{\mathrm{T}}\boldsymbol{V}_{\mathrm{T}}, \tag{1}$$

where $\boldsymbol{V}_{\mathrm{W}}(m_1\times 1)$ is the control vector for the woofer DM and $\boldsymbol{V}_{\mathrm{T}}(m_2\times 1)$ is the control vector for tweeter DM. The allocation of the slope $\boldsymbol{g}$ is very important to get efficient cooperation of the dual DMs. Hu *et al.* successfully distributed the lower order aberration to the woofer and the high-order aberration to the tweeter through a Zernike mode decomposition algorithm.[10] However, the orders' choice of the Zernike mode will influence the compensation ability of the dual DMs. As a matter of fact, we can distribute the wave-front slope according to the compensation ability of woofer and avoid the process of the wave-front reconstruction by Zernike mode. For the woofer DM, we can get a symmetric matrix $\boldsymbol{C}_{\mathrm{W}}(m_1\times m_1)$ through the response matrix $\boldsymbol{D}_{\mathrm{W}}$ using

$$\boldsymbol{C}_{\mathrm{W}}=\boldsymbol{D}_{\mathrm{W}}^{\mathrm{T}}\boldsymbol{D}_{\mathrm{W}}/2n, \tag{2}$$

where $\boldsymbol{C}_{\mathrm{W}}$ describes the correlation of influence slopes of different actuator. Singular value decomposition for $\boldsymbol{C}_{\mathrm{W}}$ is written as

$$\boldsymbol{C}_{\mathrm{W}}=\boldsymbol{U}\boldsymbol{S}\boldsymbol{U}^{\mathrm{T}}, \tag{3}$$

where $\boldsymbol{S}(m_1\times m_1)$ is a diagonal matrix with the singular value of $\boldsymbol{C}_{\mathrm{W}}$, $\boldsymbol{U}(m_1\times m_1)$ is a unitary matrix that consists of eigenvector of $\boldsymbol{C}_{\mathrm{W}}$, and $\boldsymbol{U}^{-1}=\boldsymbol{U}^{\mathrm{T}}$. A slope-based orthogonal basis $\boldsymbol{M}_{\mathrm{W}}(2n\times m_1)$ for woofer can be achieved from

$$\boldsymbol{M}_{\mathrm{W}}=\boldsymbol{D}_{\mathrm{W}}\boldsymbol{U}. \tag{4}$$

Note that the column vector of $\boldsymbol{M}_{\mathrm{W}}$ is orthogonal and corresponding to eigen mode of woofer DM. What is more, the eigen mode of the woofer DM is similar with the Zernike mode, of which the spatial frequency is gradually increasing with the mode's order increasing. So the portion of wave-front slop $\boldsymbol{g}_{\mathrm{w}}$ corrected by woofer could be written as

$$\boldsymbol{g}_{\mathrm{w}}=\boldsymbol{M}_{\mathrm{W}}\boldsymbol{r}=\boldsymbol{D}_{\mathrm{W}}\boldsymbol{v}_{\mathrm{w}}. \tag{5}$$

Here, $\boldsymbol{r}(m_1\times 1)$ is the coefficient for $\boldsymbol{M}_{\mathrm{W}}$, and the relation between $\boldsymbol{r}$ and $\boldsymbol{v}_{\mathrm{w}}$ is described as

$$\boldsymbol{v}_{\mathrm{w}}=\boldsymbol{U}\boldsymbol{r},\quad \boldsymbol{r}=\boldsymbol{U}^{\mathrm{T}}\boldsymbol{v}_{\mathrm{w}}. \tag{6}$$

According to Eqs. (5) and (6), we can distribute low spatial frequency and large stroke aberration to woofer DM by

$$\boldsymbol{r}=\boldsymbol{M}_{\mathrm{W}}^{+}\boldsymbol{g}, \tag{7}$$

$$\boldsymbol{v}_{\mathrm{w}}=\boldsymbol{U}\boldsymbol{I}_{\mathrm{w}}\boldsymbol{r}=\boldsymbol{U}\boldsymbol{I}_{\mathrm{w}}\boldsymbol{M}_{\mathrm{W}}^{+}\boldsymbol{g}. \tag{8}$$

Here $\boldsymbol{M}_{\mathrm{W}}^{+}$ is the pseudo-inverse matrix of $\boldsymbol{M}_{\mathrm{W}}$ and $\boldsymbol{I}_{\mathrm{w}}(m_1\times m_1)$ is a diagonal matrix. If the woofer is assigned to correct the ith mode, $\boldsymbol{I}_{\mathrm{w}}(ii)$ is one, and the residual elements of $\boldsymbol{I}_{\mathrm{w}}$ are zero. For example, if the woofer is used to correct the first three orders of eigen mode, $\boldsymbol{I}_{\mathrm{w}}=\mathrm{diag}(1,1,1,0,0,\ldots)$. Using the well-known digital PI controller, the actual control vector $\boldsymbol{V}_{\mathrm{W}}$ for the woofer DM can be achieved by

$$\boldsymbol{V}_{\mathrm{W}}(k+1)=pi_a\times\boldsymbol{V}_{\mathrm{W}}(k)+pi_b\times\boldsymbol{v}_{\mathrm{w}}(k), \tag{9}$$

where pi_a and pi_b are the parameters of PI controller. pi_a is usually set around 0.98 and pi_b is usually set around 0.2 in the adaptive optics system. After the correction by the woofer DM, the residual wave-front slope compensated by the tweeter DM can be solved as

$$\boldsymbol{g}_{\mathrm{t}}=\boldsymbol{g}-\boldsymbol{M}_{\mathrm{W}}(\boldsymbol{I}_{\mathrm{w}}\boldsymbol{M}_{\mathrm{W}}^{+}\boldsymbol{g}). \tag{10}$$

At the same time, the compensation $\boldsymbol{v}_{\mathrm{t}}$ can be calculated by

$$\boldsymbol{v}_{\mathrm{t}}=\boldsymbol{D}_{\mathrm{T}}^{+}\boldsymbol{g}_{\mathrm{t}}, \tag{11}$$

where $\boldsymbol{D}_{\mathrm{T}}^{+}$ is the pseudo-inverse matrix of $\boldsymbol{D}_{\mathrm{T}}$. The actual control vector $\boldsymbol{V}_{\mathrm{T}}$ for the tweeter DM is solved with a digital PI controller as

$$\boldsymbol{V}_{\mathrm{T}}(k+1)=pi_a\times\boldsymbol{V}_{\mathrm{T}}(k)+pi_b\times\boldsymbol{v}_{\mathrm{t}}(k), \tag{12}$$

Since the actual control vector $\boldsymbol{V}_{\mathrm{W}}$ and $\boldsymbol{V}_{\mathrm{T}}$ for the dual DMs has been obtained, there is a potential problem that the tweeter DM could generate a little shape cross-coupling with the woofer DM. To avoid this phenomenon, Liu *et al.* constructed a constraint matrix to reset control vector $\boldsymbol{V}_{\mathrm{T}}$.[11] However, the process of constructing the constraint matrix must use the Zernike mode and influence function of tweeter, as we know that the Zernike mode is a theoretical value and the precise influence function need be measured by interferometer rather than Hartmann. Compared with the method proposed by Liu *et al.*, the construction of constraint matrix $\boldsymbol{D}_{\mathrm{C}}$

only needs to use $\boldsymbol{M}_{\mathrm{W}}$ and $\boldsymbol{D}_{\mathrm{T}}$ which are easy to be measured by Shack–Hartmann, as

$$\boldsymbol{D}_{\mathrm{C}}(i,j) = k\frac{\sum_{x=1}^{2n}\boldsymbol{D}_{\mathrm{T}}(x,i)\boldsymbol{M}_{\mathrm{W}}(x,j)}{\sum_{x=1}^{2n}\boldsymbol{M}_{\mathrm{W}}(x,j)\boldsymbol{M}_{\mathrm{W}}(x,j)}, \tag{13}$$

$$\begin{bmatrix}\boldsymbol{I}\\ \boldsymbol{D}_{\mathrm{C}}\end{bmatrix}\boldsymbol{V}_{\mathrm{T}} = \boldsymbol{C}\boldsymbol{V}_{\mathrm{T}} = \begin{bmatrix}\boldsymbol{V}_{\mathrm{T}}\\ 0\end{bmatrix}, \tag{14}$$

where $\boldsymbol{D}_{\mathrm{C}}(i,j)$ is the relation coefficient between the i-th column of $\boldsymbol{D}_{\mathrm{T}}$ and the j-th column of $\boldsymbol{M}_{\mathrm{W}}$, k is an empirical parameter used to adjust the constraint intensity to the tweeter DM, and it should be set according to the relation between influence slope matrix $\boldsymbol{D}_{\mathrm{T}}$ and orthogonal basis $\boldsymbol{M}_{\mathrm{W}}$. A larger k will enhance the elimination of low order components in the surface shape of the tweeter, but the correction qualities of higher order phase aberrations will be decreased. Thus k should be carefully chosen to make a better compromise. The control vector $\boldsymbol{V}_{\mathrm{T}}$ can be reset by

$$\boldsymbol{V}_{\mathrm{T}}' = \begin{bmatrix}\boldsymbol{I}\\ \boldsymbol{D}_{\mathrm{C}}\end{bmatrix}^{+}\begin{bmatrix}\boldsymbol{V}_{\mathrm{T}}\\ 0\end{bmatrix} = \boldsymbol{C}^{+}\begin{bmatrix}\boldsymbol{V}_{\mathrm{T}}\\ 0\end{bmatrix}, \tag{15}$$

and the final control vector $\boldsymbol{V}_{\mathrm{T}}'$ for the tweeter DM will not be confined to generate cross-coupling shape with the woofer DM.

3. Numeral simulation

3.1. Construction of slope-based orthogonal basis

As described above, it is known that the key of the algorithm we proposed is to construct a slope-based orthogonal basis $\boldsymbol{M}_{\mathrm{W}}$ by the response matrix of woofer. In order to get $\boldsymbol{M}_{\mathrm{W}}$, an adaptive optics system with dual DMs is simulated. In the numerical model, the woofer is a DM with 19-actuators, and the tweeter is a DM with 127-actuators. The configuration of DM's actuators and the Shack–Hartmann wave-front sensor's sub-apertures are shown in Fig. 2.

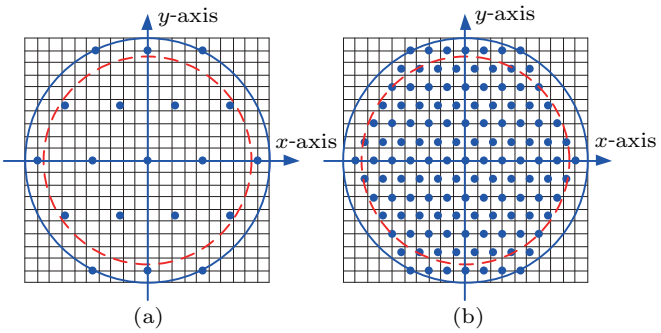


Fig. 2. (color online) Configuration of DM's actuators and the Shack–Hartmann wave-front sensor's sub-apertures: (a) woofer and (b) tweeter.

According to Fig. 2(a), the response matrix $\boldsymbol{D}_{\mathrm{W}}$ of woofer can be measured, and the slope-based orthogonal basis $\boldsymbol{M}_{\mathrm{W}}$ can be achieved through Eqs. (2)–(4). The correlation of the column vector of $\boldsymbol{M}_{\mathrm{W}}$ is shown in Fig. 3.

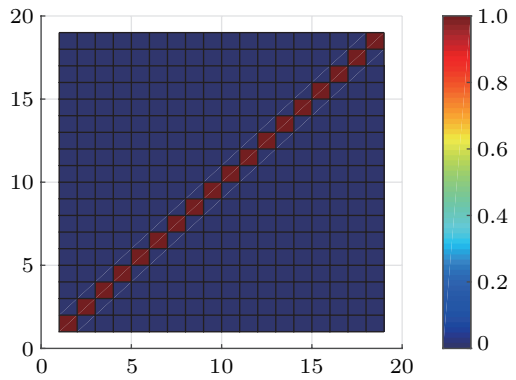


Fig. 3. (color online) Correlation of the column vector of $\boldsymbol{M}_{\mathrm{W}}$.

From Fig. 3, it is shown that the column of $\boldsymbol{M}_{\mathrm{W}}$ is completely orthogonal. What is more, the column corresponding to eigen mode can be calculated by

$$\boldsymbol{E} = \boldsymbol{W}\boldsymbol{U} = \begin{bmatrix}W_1 & W_2 & \cdots & W_{m_1}\end{bmatrix} \times \begin{bmatrix}U_{11} & U_{12} & \cdots & U_{1m_1}\\ U_{21} & U_{22} & \cdots & U_{2m_1}\\ \vdots & \vdots & \cdots & \vdots\\ U_{m_1 1} & U_{m_1 2} & \cdots & U_{m_1 m_1}\end{bmatrix}, \tag{16}$$

where W_i is the influence function of the ith actuator of woofer and $\boldsymbol{E} = \begin{bmatrix}E_1 & E_2 & \cdots & E_{m_1}\end{bmatrix}$ is the eigen mode corresponding to the column vector of $\boldsymbol{M}_{\mathrm{W}}$. The shape of the eigen mode is shown in Fig. 4.

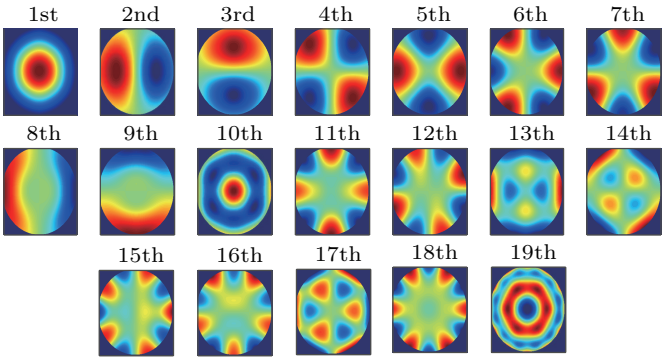


Fig. 4. (color online) Eigen mode corresponding to the column of $\boldsymbol{M}_{\mathrm{W}}$.

From Figs. 3 and 4, it indicates that $\boldsymbol{M}_{\mathrm{W}}$ is a slope-based orthogonal basis and the corresponding eigen mode is similar with the Zernike mode, of which the spatial frequency is gradually increasing with the mode's order increasing. So we can selectively distribute the large-amplitude low-order aberration to woofer DM and the remaining aberration to tweeter DM with the slope-based orthogonal basis.

3.2. Wave-front correction results

After getting the slope-based orthogonal basis M_{W}, in order to verify the validity of the algorithm described in this paper, three initial aberrations are generated from the first 50 Zernike polynomials and completely removed the tip/tilt in the simulation, because they are often corrected by the tip–tilt mirror. To make the best of the woofer compensation ability, the matrix $\boldsymbol{I}_{\mathrm{W}}$ is set as a unit matrix. Three different aberrations are described as Figs. 5(a1)–5(a3), and the correction results by the algorithm we proposed are shown in Fig. 5.

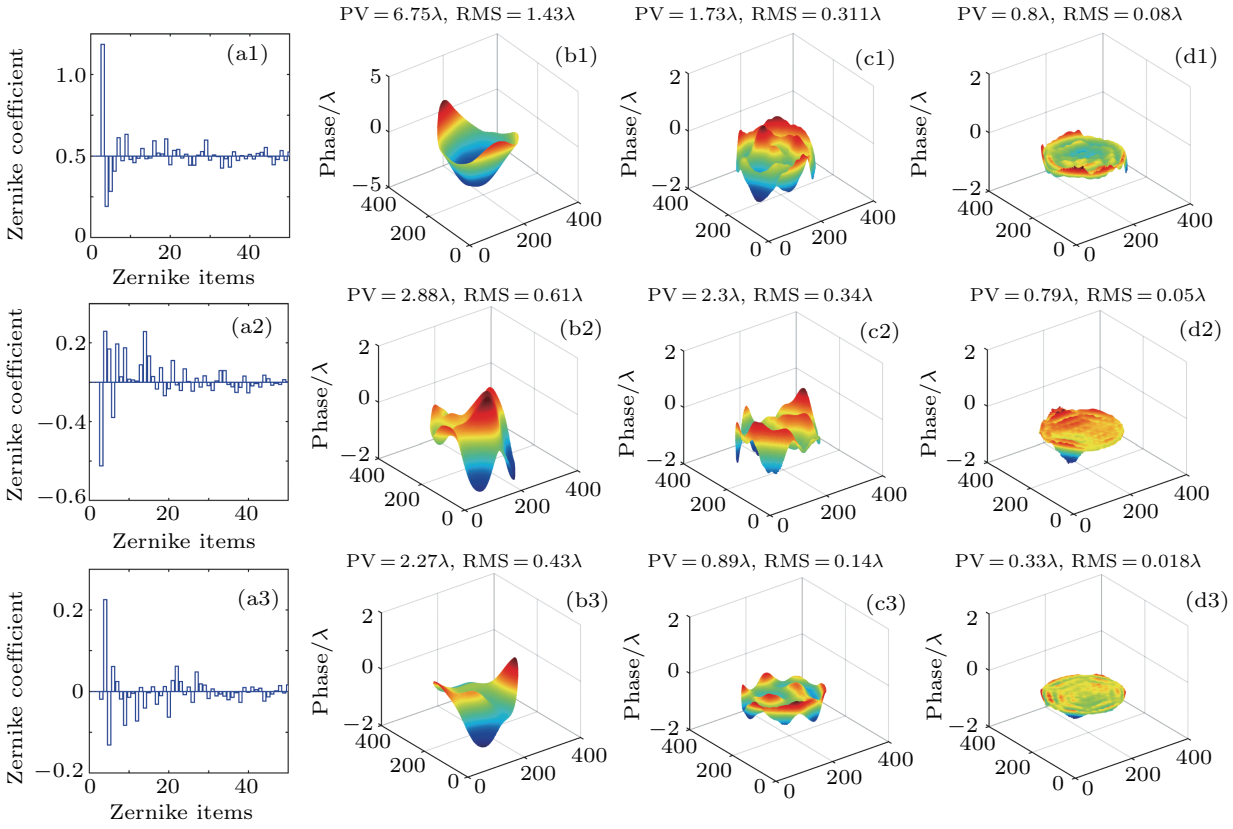


Fig. 5. (color online) Correction results in three different aberrations.

Figures 5(b1)–5(b3) show that most of the initial wave-front is corrected by the woofer, and the rest wave-front after woofer is a high spatial frequency and low stroke aberration which is compensated well by the tweeter as shown in Figs. 5(c1)–5(c3). Figures 5(d1)–5(d3) indicate that this algorithm can simultaneously control the dual DMs well, and the final RMSs of the residual wave-front are 0.08λ, 0.05λ, and 0.018λ, respectively. At the same time, to evaluate the coupling error between woofer and tweeter, a compensation ratio c of woofer as defined in

$$c = \frac{\int \emptyset_{\mathrm{wc}} \emptyset_{\mathrm{w}} \,\mathrm{d}s}{\int \emptyset_{\mathrm{w}} \emptyset_{\mathrm{w}} \,\mathrm{d}s}, \tag{17}$$

where $\emptyset_{\mathrm{w}}$ is the aberration distributed to woofer and $\emptyset_{\mathrm{wc}}$ is the aberration corrected by woofer. It is obvious that the compensation ratio c is one when $\emptyset_{\mathrm{w}}$ is completely corrected by woofer, and tweeter does not generate the cross-couple compensation to woofer.

Figure 6 shows that woofer almost compensates all the aberration distributed to it and the compensation ratios are respectively 0.996, 0.9774, and 0.981 corresponding the aberration described as Figs. 5(a1)–5(a3). It indicates that the algorithm proposed in this paper can restrain the coupling error well. According to Eq. (8), we can also distribute phase aberration to the woofer by setting the diagonal elements of $\boldsymbol{I}_{\mathrm{W}}$. With the same initial wave-front, the 1st, 10th, and 19th diagonal elements of $\boldsymbol{I}_{\mathrm{W}}$ are set as one, the correction result and performance of restraining coupling error is shown in Fig. 7.

From Figs. 7(a)–7(c), it shows that the correction of woofer does not contain other content except the 1st, 10th, and 19th, and the compensation ratios are respectively 0.98, 0.965, and 0.99, as shown in Fig. 7(d). It indicates that the aberration allocated to woofer can consist of the linear combination of the eigen modes. However, it should be noted that the lower spatial frequency aberration should be distributed to the woofer as far as possible, otherwise the correction ability of the dual DMs will decline because of the inappropriate aberration allocation as shown in the Fig. 7(d) where the RMSs of the residual wave-front are 0.1λ, 0.065λ, and 0.028λ, respectively.

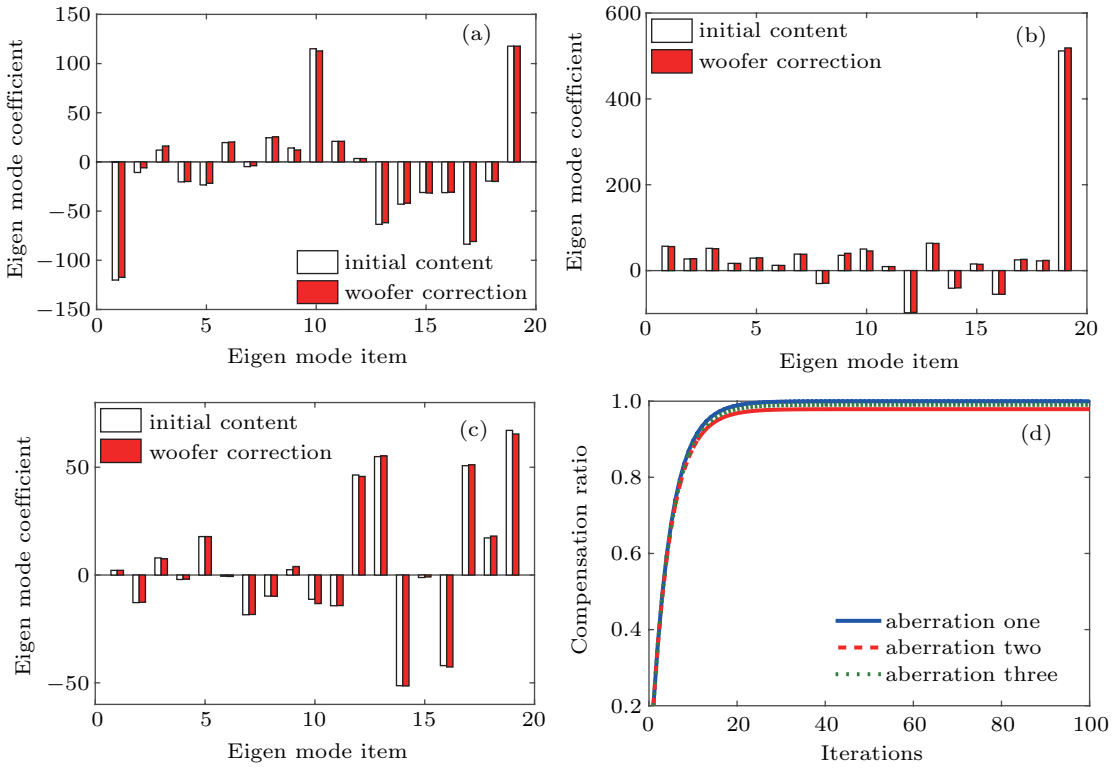


Fig. 6. (color online) Coupling error in three different aberrations.

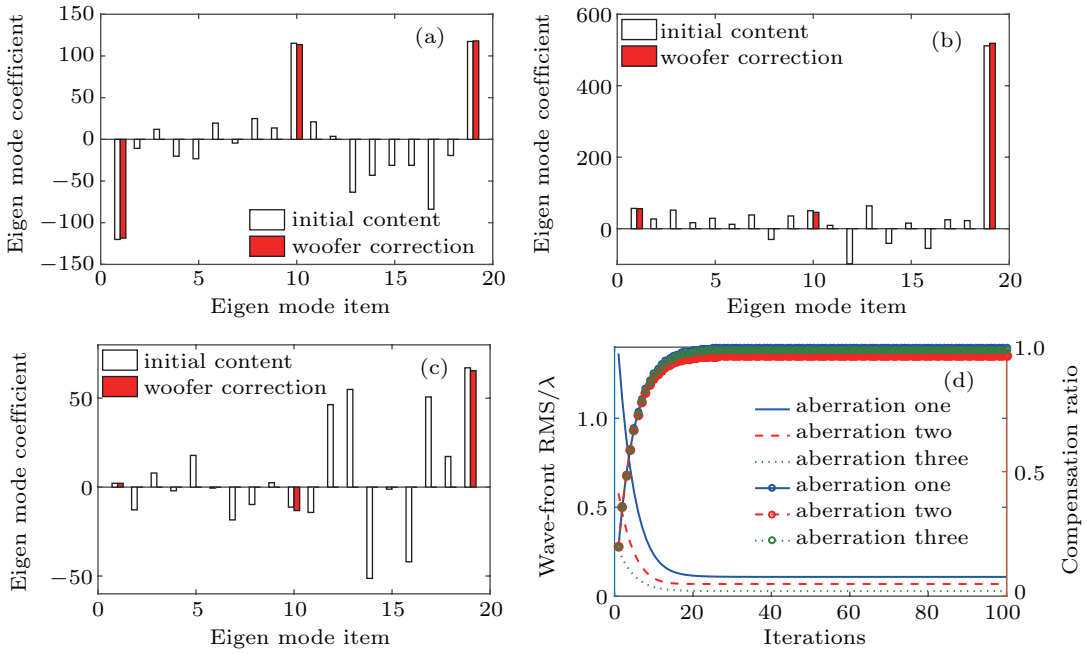


Fig. 7. (color online) Coupling error and correction results with different aberration distribution.

4. Discussion

Though many algorithms have been proposed to control the adaptive optics system with dual DMs, the algorithm that can effectually correct the aberration and suppress the coupling errors between the two DMs is very few, such as Zernike mode decomposition algorithm proposed by Liu *et al.*[11] At this moment, we make a detailed comparison of performance between the two algorithms: (a) the algorithm proposed in this paper and (b) Zernike mode decomposition algorithm proposed by Liu *et al.* Note that the algorithm (b) described as following always makes the woofer correct the first five orders of aberrations of Zernike mode, and the reconstruction matrix of the algorithm (b) is also constructed by the first 50 Zernike polynomials.

4.1. Correction capability

According to the theory of algorithm (b), it is known that algorithm (b) distributes aberration to the two DMs by choosing suited Zernike mode. But this way cannot flexibly distribute the wave-front to the dual DMs and reduce the correction capability of the dual DMs when some orders of aberrations not distributed to woofer become worse especially. In order to testify this viewpoint, a general aberration, which consists of the first 50 Zernike modes and is satisfied with Kolmogorov atmospheric turbulence, is firstly used to compare the correction performance of algorithms (a) and (b). The Zernike coefficient of initial aberration and correction results of algorithms (a) and (b) are shown in Fig. 8.

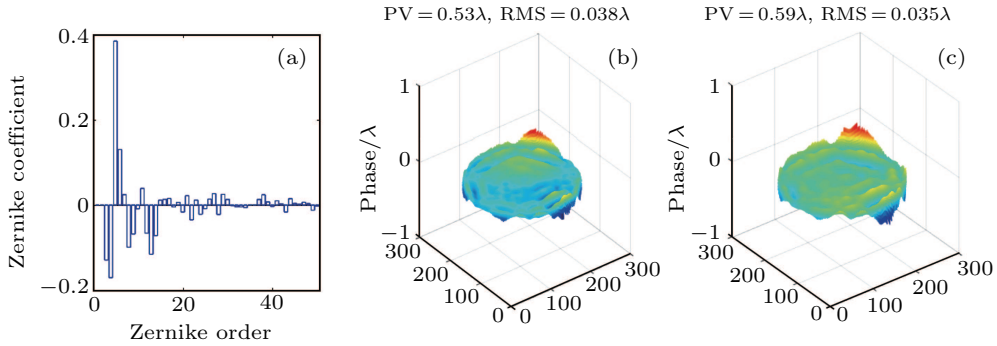


Fig. 8. (color online) Comparison of correction ability of algorithms (a) and (b) for general aberration.

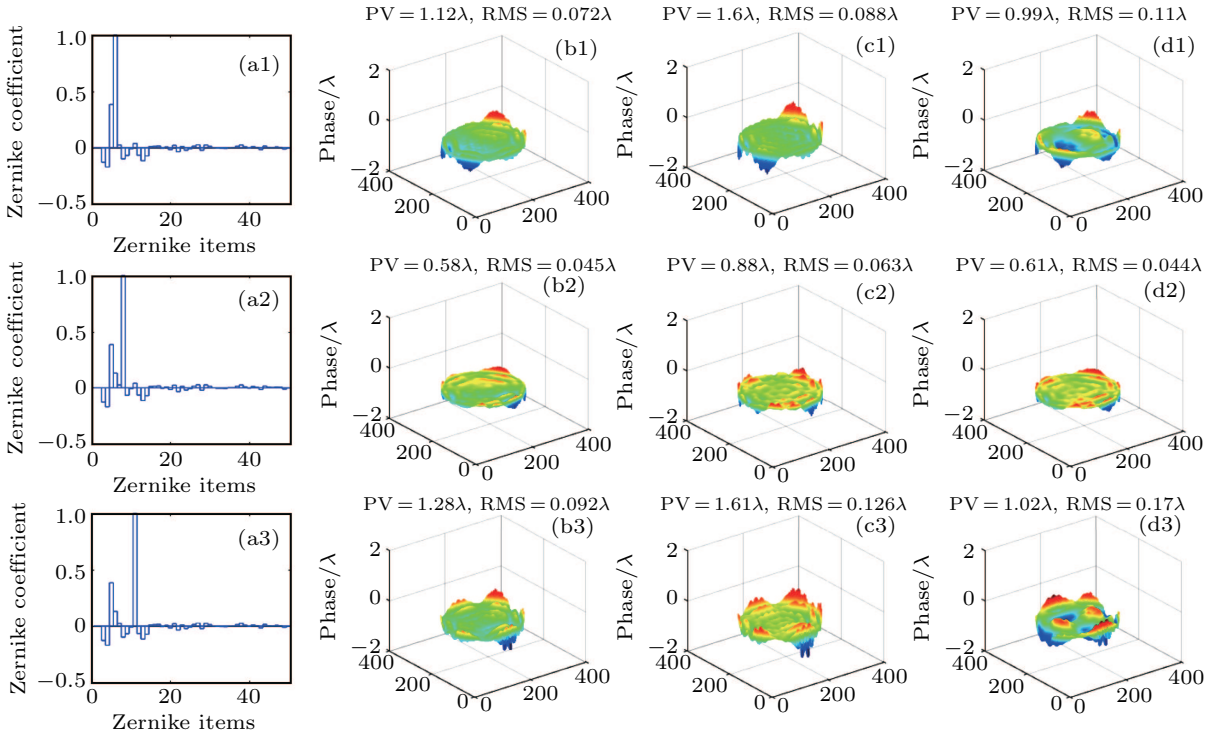


Fig. 9. (color online) Comparison of correction ability of two algorithms when some orders of aberrations become worse.

The RMSs of residual aberration corrected by algorithms (a) and (b) are respectively 0.038λ and 0.035λ as shown in Figs. 8(b) and 8(c), which means that the two algorithms have similar correction ability for general aberration. However, when some orders of aberrations become worse, for example, when the 6th, 8th, and 11th order coefficients of Zernike mode are increased to 1 as shown in Figs. 9(a1)–9(a3), the RMSs of residual aberration corrected by algorithm (a) are respectively 0.072λ, 0.045λ, and 0.092λ as shown in Figs. 9(b1)–9(b3), while the RMSs of residual aberration corrected by algorithm (b) are respectively 0.088λ, 0.063λ, and 0.126λ as shown in Figs. 9(c1)–9(c3). It is obvious that the correction results of algorithm (b) are worse than that of algorithm (a) when some orders of aberrations not distributed to woofer increase. In order to further compare the correction ability of the two algorithms, to the three initial aberrations as shown Figs. 9(a1)–

9(a3), when the 6th, 8th, and 11th orders of Zernike modes are respectively distributed to woofer in the algorithm (b), the RMSs of residual aberration are respectively 0.11λ, 0.044λ, and 0.17λ as shown in Figs. 9(d1)–9(d3). Figures 9(d1)–9(d3) show that the algorithm (b) just has similar correction ability with algorithm (a) when 8th order of Zernike mode is distributed to woofer, but has worse correction result than algorithm (a) when 6th and 11th Zernike modes are respectively distributed to woofer. The reason for this phenomenon is that 19-actuators woofer has good compensation ability for the 8th Zernike mode and has poor compensation ability for the 6th and 11th Zernike modes. Therefore, the comparison results of Fig. 9 indicates that algorithm (b) cannot flexibly distribute the wave-front to the dual DMs through Zernike mode decomposition, while algorithm (a) has better correction performance than algorithm (b) when some orders of aberrations not distributed to woofer increase.

In addition, four sets of continuous-dynamic aberrations as shown in Fig.10 are used to compare the correction performance of the two algorithms. The initial aberration shown in Fig. 10 is a set of continuous-dynamic aberration confirmed to the Kolmogorov atmospheric turbulence and generated with the simulation condition that telescope diameter D is 2 m, wind speed V is 3 m/s, sample frequency is 500 Hz, and the Fried parameter r_0 is 5 cm. Figure 10(a) shows that the two algorithms have similar correction ability for the general aberration satisfied with Kolmogorov turbulence. However, if we also set the 6th, 8th, and 11th order coefficients of the general aberration in Fig. 10(a) to 1, the algorithm (a) would have better compensation ability than algorithm (b) as shown in Figs. 10(b)–10(d). At the same moment, to the three continuous-dynamic aberrations as shown in Figs. 10(b)–10(d), when the 6th, 8th, and 11th orders of Zernike modes are respectively distributed to woofer in the algorithm (b), the RMSs of residual aberration are respectively shown in Figs. 10(b)–10(d). Figures 10(b)–10(d) show that the algorithm (b) just has similar correction ability with algorithm (a) when 8th order of Zernike mode is distributed to woofer, but has worse correction result than algorithm (a) when 6th and 11th Zernike modes are respectively distributed to woofer.

According to the comparison of Figs. 9 and 10, it can be concluded that the two algorithms have the same compensation ability for general aberration satisfied with Kolmogorov turbulence, and the algorithm (a) will have better correction ability than algorithm (b) when some order coefficients of general aberration increase. The reason for this phenomenon is that the Zernike mode decomposition for algorithm (b) cannot reasonably distribute aberration to the dual DMs, while algorithm (a) can take full use of the correction ability of woofer and release the stroke of tweeter. The stroke of tweeter actuators of algorithms (a) and (b) can be tested by

$$\mathrm{SM}_i = \frac{v_{\max} - |v_i|}{v_{\max}}, \tag{18}$$

where v_i is the voltage of ith actuator of tweeter, $v_{\max}$ is the max voltage corresponding to the max stroke, and SM_i is the saturation margin of ith actuator of tweeter. Corresponding to the correction results shown in Figs. 8 and 9, the saturation margins of tweeter's actuator of two algorithms are shown in Fig. 11.

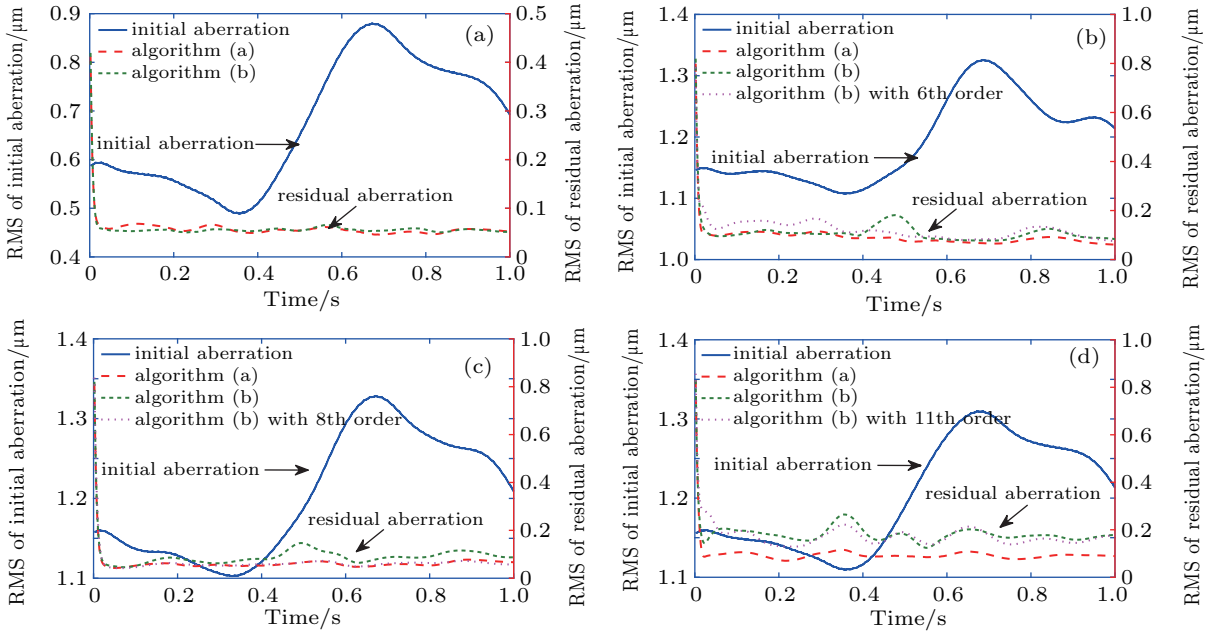


Fig. 10. (color online) Comparison of correction ability of two algorithms in different continuous-dynamic aberrations.

Figure 11(a) shows that the saturation margins of the two algorithms just have a few differences for the general aberration as shown in Fig. 8(a). But when some orders of aberrations increase, the saturation margin of algorithm (b) would decline quickly and even make some actuators saturate as shown in Fig. 11(d). It means that algorithm (b) is easier to make the tweeter actuators saturate when some orders of aberrations become larger, and then lose some compensation ability according with the result shown in Figs. 9 and 10.

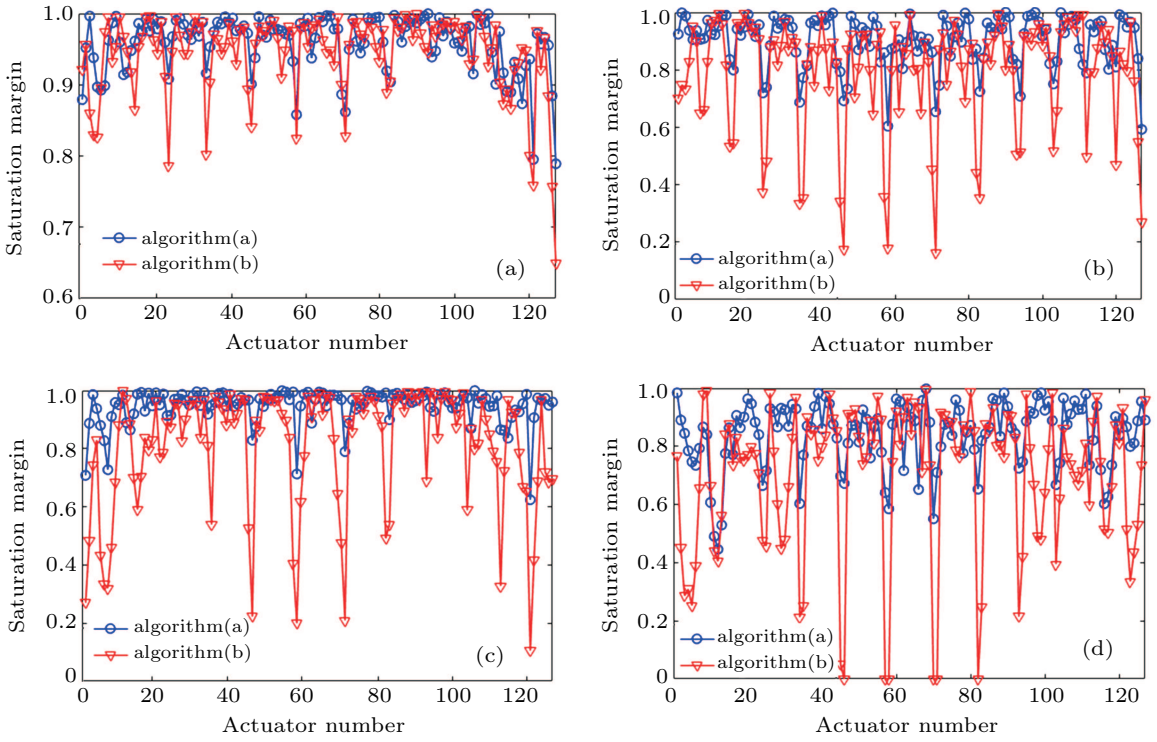


Fig. 11. (color online) Saturation margins of tweeter actuators.

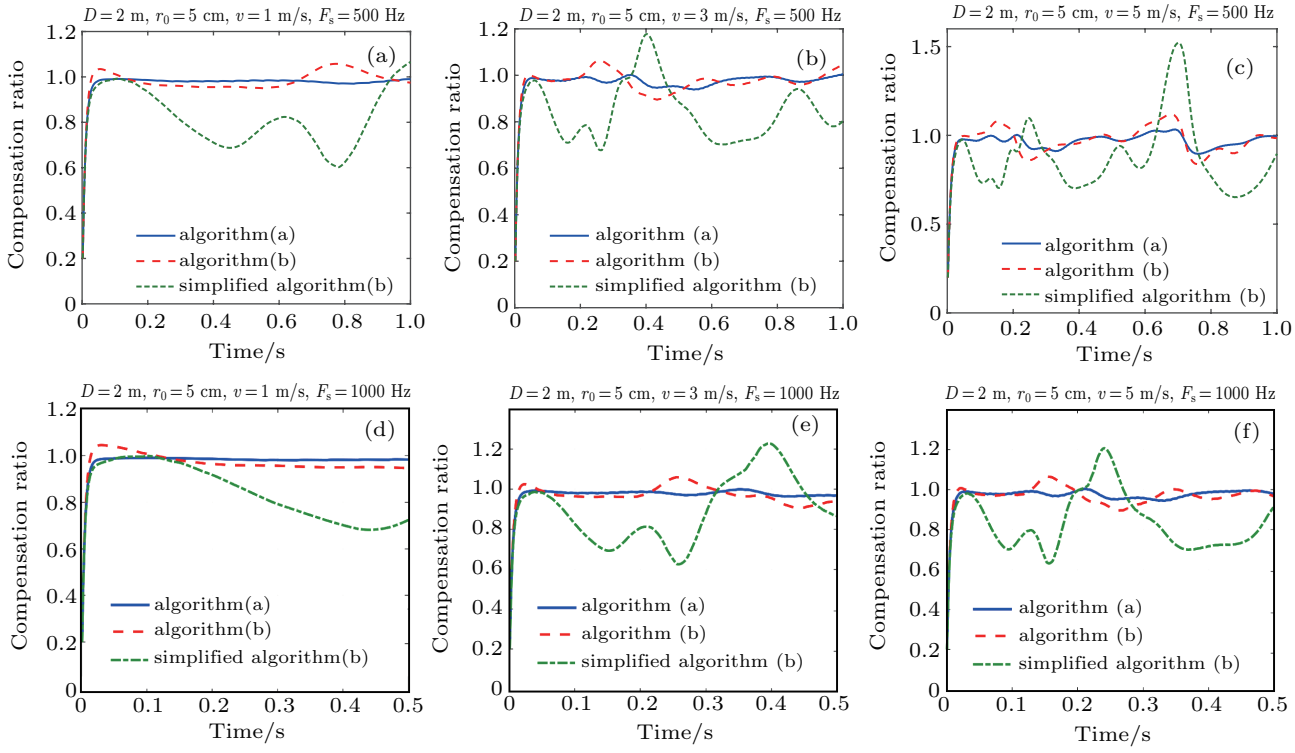


Fig. 12. (color online) Comparison of restraining the coupling error.

4.2. Coupling error

About suppressing the coupling error between the dual DMs, it is known that the two algorithms restrain the coupling error between the two DMs by constructing a constraint matrix $\boldsymbol{D}_{\mathrm{C}}$. However, the construction of the constraint matrix $\boldsymbol{D}_{\mathrm{C}}$ must use the theoretical value of Zernike mode and the influence function of tweeter's actuators in the algorithm (b).[11] If we want to get a good performance by the algorithm (b), the influence function of tweeter's actuators must be accurately measured by the interferometer or fitted by Zernike mode before calculating $\boldsymbol{D}_{\mathrm{C}}$. This process of measuring the influence function of tweeter is inconvenient. If the construction of the constraint matrix $\boldsymbol{D}_{\mathrm{C}}$ is directly using the measured slope corresponding to tweeter's actuator, the performance of suppressing the coupling error is declining evidently through this simplified algorithm (b). The comparison of restraining the coupling error between three algorithms is made in six sets of continuous-dynamic aberrations, and the result are shown in Fig. 12.

From Fig. 12, it is obvious that the simplified algorithm (b) cannot restrain the coupling error between the dual DMs with aberration changing, which means that the Zernike theory mode and influence function of tweeter's actuator are indispensable for algorithm (b) despite the fact that this process is inconvenient. Figure 12 also shows that the performance of restraining coupling error of algorithms (a) and (b) would recede with the addition of wind speed at the same sample frequency, and this problem can be improved by improving the sample frequency. In addition, the variation of compensation ratio of algorithm (a) is always smaller than algorithm (b) with the aberration changing, which indicates that algorithm (a) can keep better performance for restraining coupling error than algorithm (b).

5. Conclusion

We propose a slope-based decoupling algorithm to simultaneously control the dual DMs in woofer–tweeter adaptive optics system. This algorithm can directly use the measured slope corresponding to woofer' actuators to construct a slope orthogonal basis, and then selectively distribute the residual slope measured by Shack–Hartmann to the dual DMs and construct a constraint matrix to stop the tweeter from generating cross-couple with woofer according to the slope orthogonal matrix. Numeral simulation demonstrates that this algorithm has a good performance to simultaneously control the adaptive optics system with dual DMs. Compared with the typical decoupling algorithm, this algorithm can get better compensation ability by releasing the stroke of tweeter actuators when some high-order content of initial aberration increases. More importantly, it is convenient to construct the constraint matrix used to restrain coupling error and can keep better performance of restraining the coupling error with the continuous-dynamic aberration.

Acknowledgment

The authors would like to thank Professor Wenhan Jiang for his critical comments and thoughtful suggestions.

References

[1] Wu Z Z, Zhang Z, Kong X H, Wu J Q, Wang T, Liu M and Xie S R 2017 *Chin. Phys. B* **26** 074201
[2] Xuan L, He B, Hu L F, Li D Y, Xu H Y, Zhang X Y, Wang S X, Wang Y K, Yang C L, Cao Z L, Mu Q Q and Lu X H 2016 *Chin. Phys. B* **25** 094216
[3] Lu J, Li H, He Y, Shi G H and Zhang Y D 2011 *Acta Phys. Sin.* **60** 034207 (in Chinese)
[4] Dagel D J, Cowan W D, Spahn O B, Grossetete G D and Griñe A J 2005 *J. Microelectro-Mech. Syst.* **15** 572
[5] Zou W, Qi X and Burns S A 2011 *Opt. Express* **2** 1986
[6] Chen D C, Jones S M, Silva D A and Olivier S S 2007 *J. Opt. Soc. Am. A* **24** 1305
[7] Zawadzki R, Choi S, Jones S M, Oliver S S and Werner J S 2007 *J. Opt. Soc. Am. A* **24** 1373
[8] Cense B, Koperda E, Brown J M, Kocaoglu O P, Gao W, Jonnal R S and Miller D T 2009 *Opt. Express* **17** 4095
[9] Conan R, Bradley C, Hampton C P, Keskin O, Hilton A and Blain C 2007 *Appl. Opt.* **46** 4329
[10] Hu S, Xu B, Zhang X, Hou J, Wu J and Jiang W H 2006 *Appl. Opt.* **45** 2638
[11] Liu W J, Dong L Z, Yang P, Lei X, Yan H and Xu B 2013 *Opt. Express* **20** 23885
[12] Lavigne J F and Véran J P 2008 *J. Opt. Soc. Am. A* **25** 2271
[13] Hampton P J, Agathoklis P, Conan R and Bradley C 2010 *J. Opt. Soc. Am. A* **27** A145
[14] Zou W, Qi X and Burns S A 2008 *Opt. Lett.* **33** 2602
[15] Zou W and Burns S A 2009 *Opt. Express* **17** 20167
[16] Zou W and Burns S A 2012 *Appl. Opt.* **51** 1198
[17] Li C H, Sredar N, Ivers K, Queener H and Porter J 2010 *Opt. Express* **18** 16671